IJAMAA: January-December 2015, Volume 10, Nos. 1-2, pp. 19-36

NUMERICAL STUDY OF MAGNETOHYDRODYNAMIC UNSTEADY NATURAL CONVECTION IN A SQUARE CAVITY WITH DIFFERENTIALLY HEATED AND COOLED VERTICAL WALLS

S. GOKILA AND V. SELLADURAI

ABSTRACT: A finite-difference method is used to study the heat-transfer response of an incompressible laminar unsteady natural convection flow in an enclosed cavity with an external magnetic field, which is applied parallel to the gravity. The two vertical side walls are partially heated and cooled, while the top wall is adiabatic and bottom wall is maintained with linear temperature variation. The governing coupled and non-linear equations are solved by more accurate, unconditionally stable and fast converging implicit finite difference scheme, namely, Alternating Direction Implicit method. Calculations have been carried out for a wide range of non-dimensional parameters, such as Grashof number, *Gr*, Hartmann number, *Ha*, and Prandtl number, Pr, to examine the results obtained. The detailed flow structure and the associated heat transfer characteristics inside the cavity are presented. The average Nusselt number, *Nu*, increases with increase in Grashof number, *Gr*, but decreases with increase in Hartmann number, *Ha*.

Keywords: Magneto convection, Square cavity, Differentially heated and cooled vertical walls, Finite difference scheme.

1. INTRODUCTION

The buoyancy driven convection in a fluid filled cavity is a topic of interest for many researchers, due to its wide range of applications in Cyrogenic Industry, Cooling problems, Crystal growth techniques, Space applications etc., Free convection arises in a fluid due to the density variations caused by the temperature differences of the system. The temperature fluctuations caused by the unsteady buoyancy driven convective flows make inhomogeneities in the crystal growth.

The first numerical study of natural convection in rectangular cavities was presented by Poots [13]. Wilkes and Churchill [18] used an implicit alternating direction finite difference method to study the natural convection of a fluid contained in a long horizontal rectangular enclosure with differentially heated vertical walls for different Grashof numbers and aspect ratios. Davis [3] studied the two dimensional natural convection in an enclosed rectangular cavity and also in a square cavity with differentially heated side walls and has suggested a bench mark solution [4]. Sathiyamoorthy *et al*., [15] presented the numerical study of natural convection flow in a closed square cavity when the bottom wall is uniformly heated and vertical walls are linearly heated whereas

the top wall is insulated. Nithyadevi *et al*., [10] studied the effect of aspect ratio on the natural convection of a fluid contained in a rectangular cavity with partially thermally active side walls.

Frederick and Quiroz [6] have remarked that the transition to convection occurs in the range of Rayleigh numbers10^3 to 10^5 in their study on transition from conduction to convection regime in a cubical enclosure with a partially heated wall. Deng *et al*., [5] numerically studied a two dimensional steady and laminar natural convection in a rectangular enclosure with discrete heat sources on walls. They have remarked that the heat source on the floor increases the thermal instability and acts as a proportional effect on convection, while the heat source on the side wall increases the thermal instability and acts as a reverse effect on convection.

Heat transfer for an electrically conducting fluid flow under the influence of a magnetic field is considered to be of significant importance due to its application in many engineering problems such as nuclear reactors and those dealing with liquid metals. In the last few decades, magnetoconvection received a great deal of attention as its multi-faceted applications in geophysics, astro-physics, engineering and industries etc. It finds applications in different areas such as aerodynamic extrusion of plastic sheets, material handling conveyors, cooling of an infinite metallic plate in a cooling bath, liquid film in condensation processes, growth of large-diameter semi-conductor crystals Numerical Study of Magnetohydrodynamic Unsteady Natural Convection, nuclear reactors, in the study of the structure of stars and planets, MHD generators and in space science, to quote a few. Some of the important applications of the influence of magnetic field on fluid flow were well documented by Crammer and Pai [2].

Earlier researchers have done work on magneto convection in biomedical problems such as developing mathematical problems for transportation of blood through artilleries, tubes, channels etc. and finding the influence of a magnetic field on the blood oxygenation process etc. Masumdar *et al*., [8] studied the flow of a viscous incompressible Newtonian fluid through a circular tube under a transverse magnetic field and determined the distribution of axial velocity and temperature in terms of the Hartmann number. This problem serves as a simple model of a physiological flow and is of high interest from the view point that externally imposed magnetic field has considerable influence on the biological system of living beings.

Several aspects of steady, free convection of an electrically conducting fluid in a magnetic field have been discussed by many researchers. (Ozoe and Maruo [11], Ozoe and Okada [12], Moreau [9], Vasseur *et al*., [16], Rudraiah *et al*., [14], Alchaar *et al*., [1] etc.,).

The MHD free convection of an electrically conducting fluid, in a rectangular enclosure of aspect ratios 1 and 2 with two side walls maintained at uniform heat flux

condition, has been studied by Venkatachalappa and Subbraya [17]. Their numerical results showed that with the application of an external magnetic field which is aligned with gravity, the temperature and velocity of the fluids are significantly modified. For sufficiently large magnetic field strength the convection was found to be suppressed for all values of the Grashof number. Kandaswamy *et al*., [7] investigated numerically magnetoconvection of an electrically conducting fluid in a square cavity with partially thermally active vertical walls.

The analysis of buoyancy driven flow in a square cavity with vertical walls each consisting of alternating equal sized hot and cold surface elements facing each other, has not received much attention. Hence, in the present study attention has been focused on the above problem and analysis is made using finite difference method. The object of present work is to extend the finite difference method to the computation of unsteady natural convection in situations in which momentum transfer is significant in two dimensions and hence gain a better understanding of the effect of magnetic field on natural convection within cavities. The two vertical walls of the enclosure are subjected to partial heating and cooling such that heated and cooled surface elements face each other in an opposed manner. The bottom wall is linearly heated and the top wall is well insulated. An external magnetic field is assumed to be applied parallel to gravity and the induced magnetic field is neglected. The numerical calculations are carried out for Grashof number varying from 500-80,000 and the magnetic parameter, the Hartmann number *Ha*, varying from 0 to 13.

The flow characteristics are depicted in terms of steady state isotherms, stream lines and velocity profiles.

2. MATHEMATICAL FORMULATION

In the present study a two dimensional square cavity of length ℓ as shown in Fig. 1 is considered. Initially at time $t = 0$, the fluid is assumed to be motionless and at a uniform

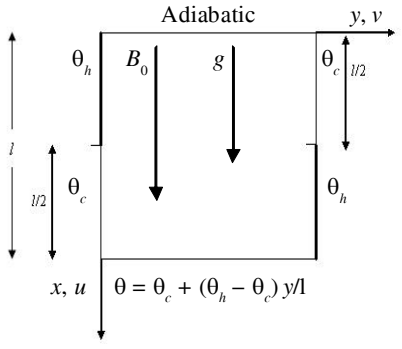

Figure 1: Schematic Diagram of the Physical System

temperature θ_0, which is equal to the average of the vertical wall temperatures. The vertical isothermal side walls of the cavity are assumed to be maintained at temperatures θ_h and θ_c, where $\theta_h > \theta_c$. It is assumed that the heated and cooled surface elements face each other in an opposed manner in the vertical direction. The top horizontal wall is assumed as insulated while the bottom horizontal wall is maintained with linear variation as $\theta = \theta_c + (\theta_h - \theta_c)\, y/\ell$. The gravitational force (g) acts in the downward direction and u and v denote the velocity components in the x and y directions respectively. A uniform magnetic field B_0 is applied parallel to the gravity and the induced magnetic field is assumed to be neglected.

The conservation equations for an unsteady laminar two dimensional flow of an electrically conducting incompressible fluid under Boussinesq approximation are given by,

$$\frac{\partial u}{\partial x} + \frac{\partial v}{\partial y} = 0 \tag{1}$$

$$\frac{\partial u}{\partial t} + u\frac{\partial u}{\partial x} + v\frac{\partial u}{\partial y} = g\beta(\theta - \theta_0) - \frac{1}{\rho}\frac{\partial p'}{\partial x} + \gamma\left(\frac{\partial^2 u}{\partial x^2} + \frac{\partial^2 u}{\partial y^2}\right) \tag{2}$$

$$\frac{\partial v}{\partial t} + u\frac{\partial v}{\partial x} + v\frac{\partial v}{\partial y} = -\frac{1}{\rho}\frac{\partial p'}{\partial y} + \gamma\left(\frac{\partial^2 v}{\partial x^2} + \frac{\partial^2 v}{\partial y^2}\right) - \frac{\sigma B_0^2 V}{\rho} \tag{3}$$

$$\frac{\partial \theta}{\partial t} + u\frac{\partial \theta}{\partial x} + v\frac{\partial \theta}{\partial y} = \frac{K}{\rho C_p}\left(\frac{\partial^2 \theta}{\partial x^2} + \frac{\partial^2 \theta}{\partial y^2}\right) \tag{4}$$

where σ denotes the electrical conductivity of the medium, $B_0 = \mu H_1$ is the magnetic field induction where H_1 is the magnetic field strength. The third term in the third equation is the magnetic ponderomotive force and is the only term appearing due to MHD effects.

The initial and boundary conditions are given by,

$$t = 0; \quad 0 \le x \le \ell; \quad 0 \le y \le \ell; \quad u = v = 0; \quad \theta = \theta_0$$

$$t > 0;$$

$$x = 0; \quad u = v = 0; \quad \frac{\partial \theta}{\partial x} = 0$$

$$x = \ell; \quad u = v = 0; \quad \theta = \theta_c + (\theta_h - \theta_c)\frac{y}{\ell}$$

$$y = 0; \quad u = v = 0; \quad \theta = \begin{cases} \theta_h & 0 \le x \le \ell/2 \\ \theta_c & \ell/2 < x \le \ell \end{cases}$$

$$y = \ell; \quad u = v = 0; \quad \theta = \begin{cases} \theta_c & 0 \le x \le \ell/2 \\ \theta_h & \ell/2 < x \le \ell \end{cases}$$

Introducing the following dimensionless variables

$$X = \frac{x}{\ell}, \quad Y = \frac{y}{\ell}, \quad U = \frac{u\ell}{\gamma}, \quad V = \frac{v\ell}{\gamma}, \quad P = \frac{p'\ell^2}{\rho\gamma^2}, \quad T = \frac{\theta - \theta_0}{\theta_h - \theta_0}, \quad \tau = \frac{t\gamma}{\ell^2}$$

$$Gr = \frac{g\beta(\theta_h - \theta_c)\,\ell^3}{\gamma^2}, \quad \Pr = \frac{\gamma}{\alpha}, \quad Ha = B_0\,\ell\sqrt{\frac{\sigma}{\mu}}$$

the above equations (1)-(4) get modified as

$$\frac{\partial U}{\partial X} + \frac{\partial V}{\partial Y} = 0 \tag{5}$$

$$\frac{\partial U}{\partial \tau} + U\frac{\partial U}{\partial X} + V\frac{\partial U}{\partial Y} = -\frac{Gr}{2}T - \frac{\partial P}{\partial X} + \frac{\partial^2 U}{\partial X^2} + \frac{\partial^2 U}{\partial Y^2} \tag{6}$$

$$\frac{\partial V}{\partial \tau} + U\frac{\partial U}{\partial X} + V\frac{\partial U}{\partial Y} = -\frac{\partial P}{\partial Y} + \frac{\partial^2 V}{\partial X^2} + \frac{\partial^2 V}{\partial Y^2} - Ha^2 V \tag{7}$$

$$\frac{\partial T}{\partial \tau} + U\frac{\partial T}{\partial X} + V\frac{\partial T}{\partial Y} = \frac{1}{\Pr}\left(\frac{\partial^2 T}{\partial X^2} + \frac{\partial^2 T}{\partial Y^2}\right) \tag{8}$$

The initial and boundary conditions are given in the non dimensional form as

$$\tau = 0; \quad 0 \le X \le 1, \quad 0 \le Y \le 1, \quad U = V = 0, \quad T = 0$$

$$\tau > 0$$

$$X = 0; \quad U = V = 0; \quad \frac{\partial T}{\partial X} = 0$$

$$X = 1; \quad U = V = 0; \quad T = 2Y - 1$$

$$Y = 0; \quad U = V = 0; \quad \theta = \begin{cases} 1 & 0 \le x \le 0.5 \\ -1 & 0.5 < x \le 1 \end{cases}$$

$$Y = 1; \quad U = V = 0; \quad T = \begin{cases} -1 & 0 \le x \le 0.5 \\ 1 & 0.5 < x \le 1 \end{cases}$$

Eliminating pressure term from the equations (6) and (7), we get

$$\frac{\partial}{\partial \tau}\left(\frac{\partial U}{\partial Y}-\frac{\partial V}{\partial X}\right)+U\frac{\partial^2 U}{\partial X\partial Y}+V\frac{\partial^2 U}{\partial Y^2}-U\frac{\partial^2 V}{\partial X^2}-V\frac{\partial^2 V}{\partial X\partial Y}$$

$$=-\frac{Gr}{2}\frac{\partial T}{\partial Y}+\frac{\partial}{\partial Y}(\nabla^2 U)-\frac{\partial}{\partial X}(\nabla^2 V)+Ha^2\frac{\partial V}{\partial X}.$$

Introducing the vorticity ς and the stream function ψ, the equations governing the problem can be written as

$$\nabla^2\psi=-\varsigma \tag{10}$$

$$U=\frac{\partial\psi}{\partial Y},\quad V=-\frac{\partial\psi}{\partial X} \tag{11}$$

$$\frac{\partial\varsigma}{\partial\tau}+U\frac{\partial\varsigma}{\partial X}+V\frac{\partial\varsigma}{\partial Y}=\frac{Gr}{2}\frac{\partial T}{\partial y}+\nabla^2\varsigma-Ha^2\frac{\partial V}{\partial X} \tag{12}$$

$$\frac{\partial T}{\partial\tau}+U\frac{\partial T}{\partial X}+V\frac{\partial T}{\partial Y}=\frac{1}{\Pr}\nabla^2 T \tag{13}$$

$\tau=0;\quad 0\le X\le 1,\quad 0\le Y\le 1,\quad \varsigma=0,\quad T=0$

$\tau>0$

$X=0;\quad \psi=\dfrac{\partial\psi}{\partial X}=0;\quad \dfrac{\partial T}{\partial X}=0$

$X=1;\quad \psi=\dfrac{\partial\psi}{\partial X}=0;\quad T=2Y-1$

$$Y=0;\quad \psi=\frac{\partial\psi}{\partial Y}=0;\quad T=\begin{cases}1 & 0\le x\le 0.5\\ -1 & 0.5<x\le 1\end{cases}$$

$$Y=1;\quad \psi=\frac{\partial\psi}{\partial Y}=0;\quad T=\begin{cases}-1 & 0\le x\le 0.5\\ 1 & 0.5<x\le 1\end{cases}$$

The local Nusselt number is $N_u=\left(\frac{\partial T}{\partial Y}\right)_{Y=0}$ and its mean value $\overline{N_u}$ over the height of the enclosure will depend on *Gr*, Pr, *Ha* and τ. For conduction the local and average Nusselt number N_u and $\overline{N_u}$ would be equal to unity.

3. FINITE DIFFERENCE APPROXIMATION

The above equations (10)-(13) are called as the stream function, velocity, vorticity and temperature equations, respectively. An approximation to their solution will be obtained at a finite number of grid points having co-ordinates $X = i\,\Delta X$ and $Y = j\,\Delta Y$ and at discrete time $T = n\,\Delta\tau$ where i, j, n are integers. The vorticity and temperature equations are parabolic while the stream function equation is elliptic.

It is assumed that all quantities are known at a time $n\,\Delta\tau$. An implicit alternating direction technique based on suitable finite difference approximations of the vorticity and temperature equations is employed to advance the fields of vorticity and temperature at the interior grid points across a time step $n\,\Delta\tau$ to the new level $(n+2)\,\Delta\tau$. At any grid point the term $\frac{\partial T}{\partial Y}$ in the vorticity equation and the coefficient velocities U and V are treated as constants over a time step. All space derivatives are given centered difference representations.

Thus the relevant finite difference approximation to the temperature equation to be used consequtively over two half time steps, each of duration $\Delta\tau/2$ are given by,

$$\frac{T_{i+1,\,j+1}^{(n+1)} - T_{i+1,\,j+1}^{(n)}}{\frac{\Delta\tau}{2}} + U_{i+1,\,j+1}^{(n)} \frac{T_{i+2,\,j+1}^{(n+1)} - T_{i,\,j+1}^{(n+1)}}{2\Delta x} + V_{i+1,\,j+1}^{(n)} \frac{T_{i+1,\,j+2}^{(n)} - T_{i+1,\,j}^{(n)}}{2\Delta y}$$

$$= \frac{1}{\mathrm{Pr}} \left[\frac{T_{i+2,\,j+1}^{(n+1)} - 2T_{i+1,\,j+1}^{(n+1)} + T_{i,\,j+1}^{(n+1)}}{\Delta x^2} + \frac{T_{i+1,\,j+2}^{(n)} - 2T_{i+1,\,j+1}^{(n)} + T_{i+1,\,j}^{(n)}}{\Delta y^2} \right]$$

followed by

$$\frac{T_{i+1,\,j+1}^{(n+2)} - T_{i+1,\,j+1}^{(n+1)}}{\frac{\Delta\tau}{2}} + U_{i+1,\,j+1}^{(n)} \frac{T_{i+2,\,j+1}^{(n+1)} - T_{i,\,j+1}^{(n+1)}}{2\Delta x} + V_{i+1,\,j+1}^{(n)} \frac{T_{i+1,\,j+2}^{(n+2)} - T_{i+1,\,j}^{(n+2)}}{2\Delta y}$$

$$= \frac{1}{\mathrm{Pr}} \left[\frac{T_{i+2,\,j+1}^{(n+1)} - 2T_{i+1,\,j+1}^{(n+1)} + T_{i,\,j+1}^{(n+1)}}{\Delta x^2} + \frac{T_{i+1,\,j+2}^{(n+2)} - 2T_{i+1,\,j+1}^{(n+2)} + T_{i+1,\,j}^{(n+2)}}{\Delta y^2} \right]. \qquad (14)$$

The above equations are implicit in the X and Y directions, respectively, and when applied to every point in a column or row, as the case may be, yield tridiagonal systems in the unknown temperature $T_{i+1,\,j+1}^{(n+1)}, T_{i+1,\,j+1}^{(n+2)}$. Similar approximation also holds for the vorticity equation. The method of successive under relaxation is then employed in conjunction with the newly computed vorticity $\varsigma_{i+1,\,j+1}^{(n+2)}$ to solve the stream function equation for the new stream function field. Thus, $\psi_{i+1,\,j+1}^{(m)}$ if denotes the approximation

at the m^{th} iteration to the stream function at a point, a further approximation $\psi_{i+1,\,j+1}^{(m+1)}$ is obtained from

$$\psi_{i+1,\,j+1}^{(m+1)} = \psi_{i,\,j}^{(m)} + \frac{\omega}{4}\left((\Delta x)^2 \varsigma_{i,\,j}^{(n+2)} + \psi_{i-1,\,j}^{(m)} + \psi_{i+1,\,j}^{(m)} + \psi_{i,\,j-1}^{(m)} + \psi_{i,\,j+1}^{(m)} - 4\psi_{i,\,j}^{(m)}\right) \quad (15)$$

where ω is the relaxation parameter.

Once the optimum value ω_{opt} of the relaxation parameter ω has been found by trial and error for a given system of grid points, this value is then employed in all further computations with that grid. The new wall vorticities are then computed by considering Taylor's series expansions for stream function in the vicinity of the walls. For example, for points (i, 1) and (i, 2), removed by one and two grid spacings, respectively, in the Y direction from a grid point (i, 0) on the left hand wall $Y = 0$, the equations obtained are

$$\psi_{i,\,1} = \psi_{i,\,0} + \frac{h}{1!}\frac{\partial \psi}{\partial Y} + \frac{h^2}{2!}\frac{\partial^2 \psi}{\partial Y^2} + \frac{h^3}{3!}\frac{\partial^3 \psi}{\partial Y^3} \quad (16)$$

$$\psi_{i,\,2} = \psi_{i,\,0} + \frac{2h}{1!}\frac{\partial \psi}{\partial Y} + \frac{2h^2}{2!}\frac{\partial^2 4}{\partial y^2} + \frac{2h^3}{3!}\frac{\partial^3 \psi}{\partial Y^3} \quad (17)$$

In the above equations (16) and (17) all derivatives are considered at the wall point (i, 0). But, from the boundary conditions both $\psi_{i,\,0}$ and $\frac{\partial \psi}{\partial Y}$ are zero. After eliminating $\frac{\partial^2 \psi}{\partial Y^2}$ and noting from the defining equation for vorticity that $\xi = -\frac{\partial^2 \psi}{\partial Y^2}$, the following approximations is obtained for vorticity at the wall.

$$\varsigma_{i,\,1,\,n+1} = -\frac{8\psi_{i,\,1} - \psi_{i,\,2}}{2(\Delta y)^2}.$$

That is, the new wall vorticities are computed from stream functions which themselves have been calculated from the new vorticity at the interior grid points.

Finally, the new fields of U and V are obtained from space centered finite-difference approximations of the velocity equations. This computational cycle is then repeated for each of the next time steps until a steady state situation is obtained, when the following convergence criteria,

$$\left|\frac{\phi_{n+1}(i,\,j) - \phi_n(i,\,j)}{\phi_{n+1}(i,\,j)}\right| \le \varepsilon$$

for temperature, vorticity and stream function have been satisfied. In the above expression, n is any time level, ε is of order 10^{-5} and ϕ represents T, ς and ψ. The numerical solutions presented in this paper were acquired from a 41×41 grid system and with a time increment of order 10^{-4}.

The ADI method has been shown to be stable (elsewhere) for any ratio of the time increment to the space increments as long as the same time increment is maintained at all levels. Prior to the present calculations, as a partial verification of the computational procedure the hydrodynamically developing flow of common fluid (linear density-temperature relation) was calculated and the results were compared with the solutions given by Wilkes and Churchill [18] and Rudraiah *et al*., [14] and are found to be in good agreement. The Table 1(a) shows average Nusselt number versus the Grashof number *Gr* and the Table 1(b) shows average Nusselt number versus the Hartmann number, *Ha*, for a low Prandtl number fluid with Pr = 0.733 in a square cavity with isothermal walls.

4. RESULTS AND DISCUSSION

The effect of magnetic field on the buoyancy driven convection of an electrically conducting fluid in a square cavity, with differentially heated and cooled vertical walls is investigated numerically.The parameters that govern the flow in this problem are the Grashof (*Gr*), Hartmann (*Ha*) and Prandtl numbers (Pr). Pr = 0.733 is considered for all computations. The flow fields and the temperature gradients inside the cavity are presented to illustrate the effect of Grashof number and Hartmann number.

4.1 Effect due to Change in Grashof Number

The Figs. 2(a) and (b) illustrates the streamlines and isotherms at *Gr* = 500 and 1000, *Ha* = 6. At *Gr* = 500 and 1000 the magnitudes of stream functions are considerably lower and the heat transfer is due to purely conduction. During conduction dominant heat transfer, the isotherms are nearly antisymmetric. The temperature contours as indicated in Fig. 3(b) (*i*) remains invariant upto *Gr* = 10000.

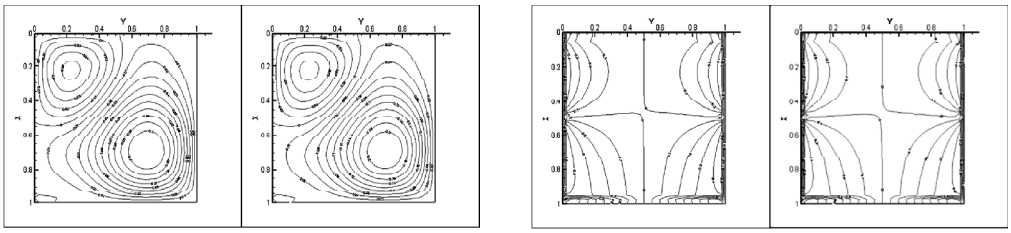

(a) Streamlines for *Gr* = 500, 1000 when *Ha* = 6

(b) Isotherms for *Gr* = 500, 1000 when *Ha* = 6

Figure 2: Clockwise and Anticlockwise Flows are Shown via Negative and Positive Signs of Streamfunctions, Respectively

The Figs. 3(a) and (b) show the streamlines and isotherms obtained for different Grashof numbers when *Ha* = 6. Maintaining hot and cold temperature regions on both the vertical walls, we observe that the fluid filled in the cavity experiences two density regions. As a result counter rotating eddies appear inside the cavity with one primary

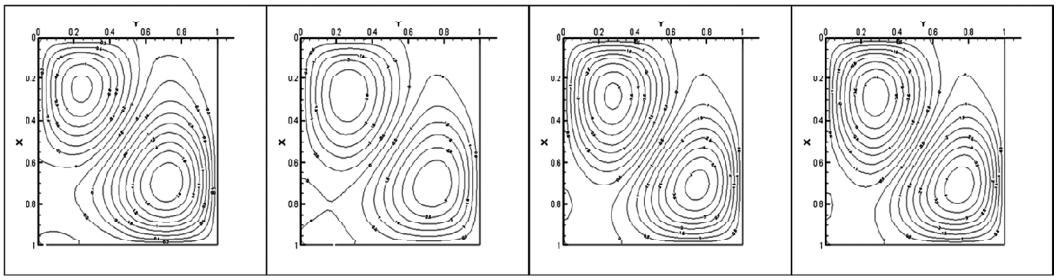

(i) $t = 0.034$ (ii) $t = 0.042$ (iii) $t = 0.495$ (iv) $t = 0.579$

(a) (i)-(iv) Steady State Stream Lines for $Gr = 10000$, $Gr = 20000$, $Gr = 26000$, $Gr = 27000$ when $Ha = 6$

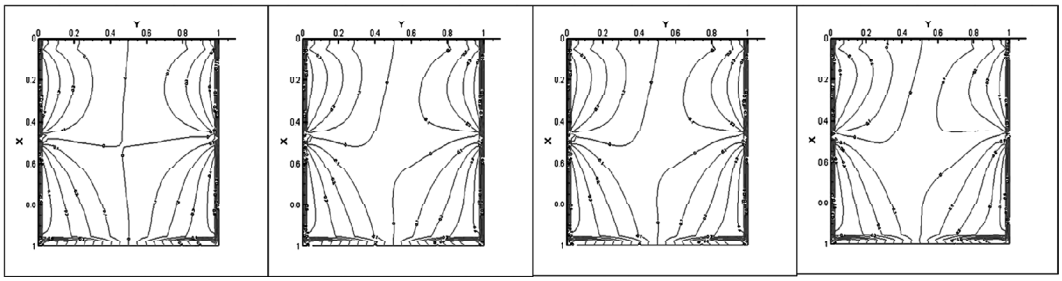

(i) $t = 0.034$ (ii) $t = 0.042$ (iii) $t = 0.495$ (iv) $t = 0.579$

(b) (i)-(iv) Steady State Isotherms for $Gr = 10000$, $Gr = 20000$, $Gr = 26000$, $Gr = 27000$ when $Ha = 6$

Figure 3: Clockwise and Anticlockwise Flows are Shown via Negative and Positive Signs of Streamfunctions, Respectively

eddy circulating near the hot location in the right bottom region and a secondary eddy appears near the hot location in the left top region. A small eddy appears in the left bottom corner of the cavity. This primary eddy is influenced significantly by the linear temperature variation in the bottom wall. (Fig. 3(a) (i))

When *Gr* is increased further from 10000 to 27000, the counter rotating eddies of almost equal size emerge inside the cavity since the density near the vertical walls with heated and cooled regions becomes almost the same as can be seen from the Figs. 3 (a) (i)-(iv). The isotherms however show a gradual departure from the conduction-dominated pattern. From Fig. 3 (a) it can be noted that value of the stream function increase as *Gr* increases, indicating that the fluid is accelerating. For Hartmann numbers varying from 0-9, and for Grashof numbers *Gr* varying from 500-40000, the flow is steady and laminar. In Figs. 4(a) and 4(b), we can observe that for $Ha = 10$ and varying *Gr* from 10000-80000 the flow field is unsteady and the presence of significant convection where the

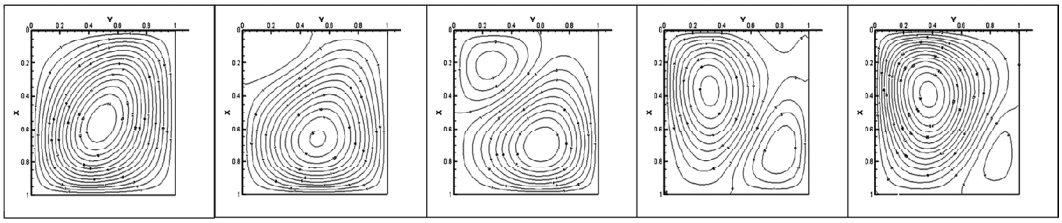

(i) $Gr = 10000$ (ii) $Gr = 25000$ (iii) $Gr = 30000$ (iv) $Gr = 70000$ (v) $Gr = 80000$

(a) (i)-(v) Unsteady State Stream Lines for $Gr = 10000$, $Gr = 25000$, $Gr = 30000$, $Gr = 70000$, $Gr = 80000$ when $Ha = 10$

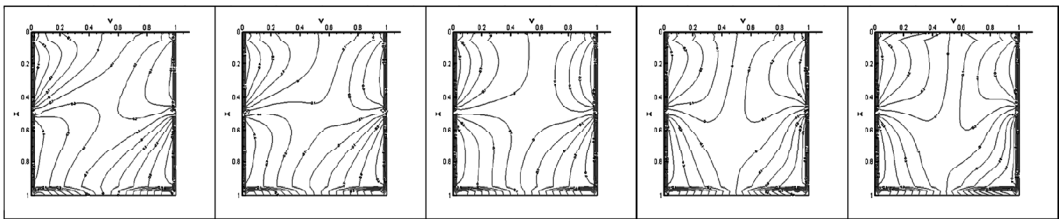

(i) $Gr = 10000$ (ii) $Gr = 25000$ (iii) $Gr = 30000$ (iv) $Gr = 70000$ (v) $Gr = 80000$

(b) (i)-(v) Unsteady State Isotherms for $Gr = 10000$, $Gr = 25000$, $Gr = 30000$, $Gr = 70000$, $Gr = 80000$ when $Ha = 10$

Figure 4: Clockwise and Anticlockwise Flows are Shown via Negative and Positive Signs of Streamfunctions, Respectively

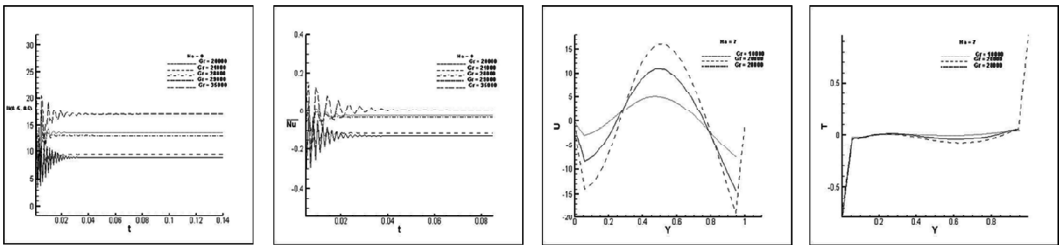

(a) (b) (c) (d)

Figure 5: (a) The Velocity *U* at Mid Point for *Gr* = 20000, *Gr* = 21000, *Gr* = 28000, *Gr* = 29000, *Gr* = 35000 when *Ha* = 9
(b) The Average Nusselt Number at Mid Point for *Gr* = 20000, *Gr* = 21000, *Gr* = 28000, *Gr* = 29000, *Gr* = 35000 when *Ha* = 9
(c) Mid Height Velocity Profiles for *Gr* = 10000, 20000, 28000 when *Ha* = 7
(d) Steady State Tempearure Profiles *Gr* = 10000, 20000, 28000 when *Ha* = 7

temperature contour starts getting deformed and pushed towards the side walls. The effect of Grashof number *Gr*, on the velocity *U*, average Nusselt number *Nu*, at the mid

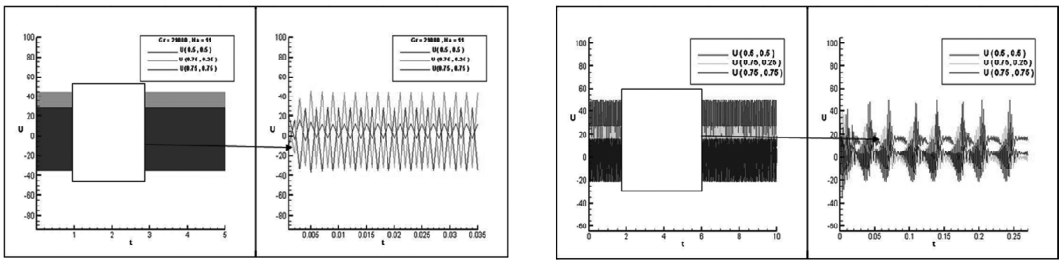

(e) (f) (g) (h)

Figure 5: (e) Unsteady Velocity Profiles *U* at Three Different Locations for *Gr* = 29000 when *Ha* = 11
(f) Shows the Flow Development in the Rectangular Region Shown in Fig. 5(e)
(g) Unsteady Velocity Profiles *U* at Three Different Locations for *Gr* = 41000 when *Ha* = 11
(h) Shows the Flow Development in the Rectangular Region Shown in Fig. 5(g)

point, mid height velocity profiles, temperature in steady state are given in Figs. 5(a)-(d). From Table 2 we observe that the average Nusselt number increases with increase in Grashof number.

4.2 Effect of Increase in External Magnetic Field Strength

From Figs. (3) and (4) we also observe that when the Grashof number is high and magnetic field is small the buoyancy-driven convection is the dominant mechanism. As magnetic field strength increases the buoyancy-driven convection is reduced. When $Ha = 11$, for any Grashof number the flow becomes unsteady and the velocity at three different locations for Grashof numbers 29000, 41000 are illustrated in Figs. 5(e) and (g). In Figs. 6(a), (b) and in Figs. 7(a), (b) the impacts due to increase in the value of Hartmann number are depicted. When the magnetic field parameter is small, the flow field consists of two counter rotating cells, and when it is increased, the flow pattern consists of a single major cell rising up along the hot wall and sinking along the cold wall of the cavity. The buoyancy force is reduced considerably. The intensities in the flow decreases owing to the increase in magnetic field. This is expected since the presence of magnetic field usually retards the flow which is observed from Table 2. The corresponding effect of the increase in magnetic field on the isotherms is that they are more straighten out since the magnetic field resists the flow and the convection is totally suppressed inside the cavity. This effect is also seen in Fig. 8(a) in which the mid height velocity profiles are flattened for higher values of the Hartmann numbers. In Fig. 8(b) the temperature profiles are depicted and in Figs. 8(c) and (d) we can also observe that the velocity at the mid point of the cavity becomes unsteady when the Hartmann numbers are increased.

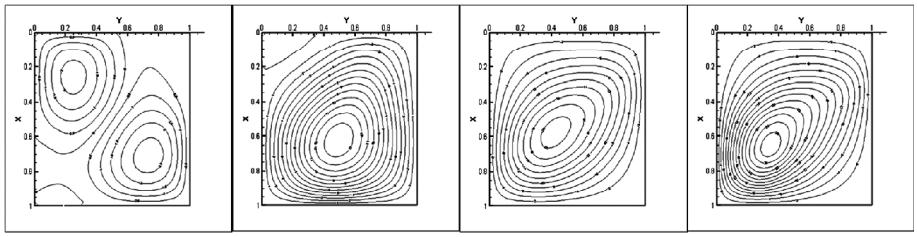

(i) (ii) (iii) (iv)

(a) (i)-(iv) Stream Lines for $Ha = 9$, $Ha = 10$, $Ha = 11$, $Ha = 13$ when $Gr = 20000$

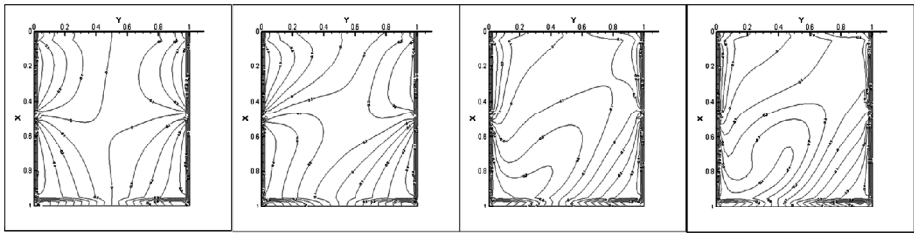

(i) (ii) (iii) (iv)

(b) (i)-(iv) Isotherms for $Ha = 9$, $Ha = 10$, $Ha = 11$, $Ha = 13$ when $Gr = 20000$

Figure 6: Clockwise and Anticlockwise Flows are Shown via Negative and Positive Signs of Streamfunctions, Respectively

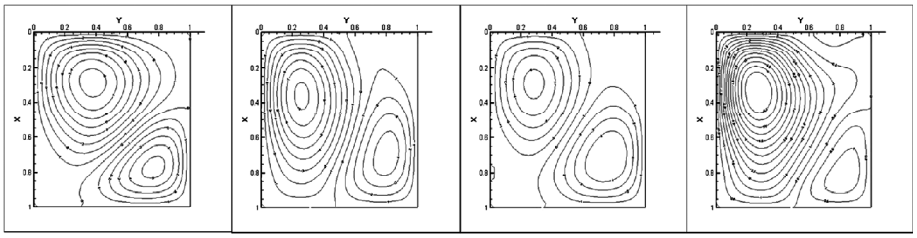

(i) (ii) (iii) (iv)

(a) (i)-(iv) Stream Lines for $Ha = 3$, $Ha = 5$, $Ha = 9$, $Ha = 11$ when $Gr = 41000$

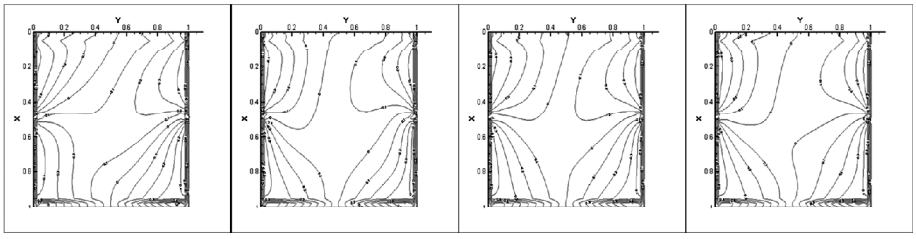

(i) (ii) (iii) (iv)

(b) (i)-(iv) Isotherms for $Ha = 3$, $Ha = 5$, $Ha = 9$, $Ha = 11$ when $Gr = 41000$

Figure 6: Clockwise and Anticlockwise Flows are Shown via Negative and Positive Signs of Streamfunctions, Respectively

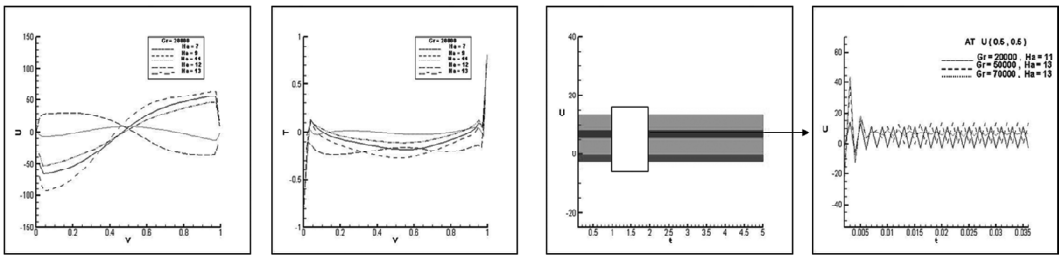

(a) (b) (c) (d)

Figure 8: (a) Mid Height Velocity Profiles for *Ha* = 7, *Ha* = 9, *Ha* = 11, *Ha* = 12, *Ha* = 13 when *Gr* = 20000
(b) Mid Height Temperature Profiles for *Ha* = 7, *Ha* = 9, *Ha* = 11, *Ha* = 12, *Ha* = 13 when *Gr* = 20000
(c) Unsteady Velocity Profiles at Mid Point for *Gr* = 20000 *Ha* = 11, *Gr* = 50000 *Ha* = 13, *Gr* = 70000 when *Ha* = 13
(d) Shows the Flow Development in the Rectangular Region Shown in Fig. 8(c)

Table 1(a)

Sl. No.	$\Delta\tau$	ΔX	ΔY	Pr	*Gr*	*Boundaey condition*	$\overline{N_u}$	$\overline{N_u}^*$	$\overline{N_u}^{**}$
1	0. 002	0. 1	0. 1	0. 733	6850	LINEAR	1. 419	1. 64	1. 5165
2	0. 001	0. 1	0. 1	0. 733	20000	LINEAR	2. 068	2. 14	1. 7833
3	0. 002	0. 1	0. 1	0. 733	20000	LINEAR	2. 068	2. 14	1. 7425
4	0. 001	0. 1	0. 1	0. 733	20000	INSULATED	2. 874	2. 14	1. 9690
5	0. 002	0. 1	0. 1	0. 733	20000	INSULATED	2. 874	2. 14	1. 9536
6	0. 001	0. 05	0. 05	0. 733	20000	INSULATED	2. 516	2. 14	3. 2258
7	0. 002	0. 1	0. 1	0. 733	20000	INSULATED	1. 286	2. 14	1. 2263

Table 1(a): Comparison of average Nusselt numbers for different Grashof numbers

$\overline{N_u}$ = Results of Wilkes and Churchill [18]

$\overline{N_u}^*$ = Results using the correlation formula given by Newell and Schmidt (1970)

$$0.18 \quad (\mathrm{Gr})^{(1/4)}\,(\mathrm{A})^{(-1/9)}, \qquad 2 \times 10^4\, Gr \le 2 \times 10^4$$

$$0.065\,(\mathrm{Gr})^{(1/3)}\,(\mathrm{A})^{(-1/9)}, \qquad 2 \times 10^5 < Gr < 2 \times 10^6$$

$\overline{N_u}^{**}$ = Present study

Table 1(b)

Gr	*Ha*	$\overline{N_u}$	$\overline{N_u}^*$
20000	1	2.4891	1.9677
	5	2.3706	2.0644
	10	2.2234	2.0233

Table 1(b): Comparison of average Nusselt numbers for different Hartmann numbers

$\overline{N_u}$ = Results of Rudraiah *et al*., [14]

$\overline{N_u}^*$ = Present study

Table 2

Gr	*Ha*	*
5000	1	−0.3331
	3	−0.3450
	5	−0.3643
	6	−0.3750
	7	−0.3858
10000	1	−0.1835
	3	−0.2004
	5	−0.2299
	6	−0.2474
	7	−0.2656
15000	1	−0.0883
	3	−0.0999
	5	−0.1253
	6	−0.1430
	7	−0.1631

Table 2: Comparison of average Nusselt numbers for different Hartmann numbers

5. CONCLUSIONS

The purpose of this work is to study numerically the two dimensional unsteady natural convection in a square cavity in the presence of magnetic field. The right and left walls of the cavity are maintained with heated and cooled portions alternatively in an opposed manner. The top wall is insulated and the bottom wall with linear temperature variation. The governing equations of motion were formulated using the vorticity – stream function approach. The code has been developed to solve the dimensionless equations using ADI method. Numerical results were obtained for a wide range of Grashof number from 500-80000, the Hartmann numbers from 0-13 for fixed Prandtl number 0.733. It is predicted that at low Hartmann numbers, from 0-9 the flow field is characterised by the presence of two counter rotating cells near the heated portions on the vertical walls moving downwards towards the centre of the cavity. As the Hartmann number is increased beyond 10, a distinctive change in the flow field occurs with one single cell which occupies the major portion of the cavity with very low stream function values. It is found that the average Nusselt number increases with increase in Grashof number but decreases with increase in Hartmann number.

6. NOTATIONS

C_p = specific heat

g = acceleration due to gravity

ℓ = side of the enclosure

Nu = Nusselt number

$\overline{N_u}$ = average Nusselt number

P' = pressure

P = dimensionless fluid pressure

Pr = Prandtl number

Gr = Grashof number

t = time

T = dimensionless temperature

u = velocity along x-direction

v = velocity along y-direction

U = velocity along X-direction

V = velocity along Y-direction

X = dimensionless distance along x-coordinate

Y = dimensionless distance along y-coordinate

Greek symbols

ΔX = grid spacing in x-dirction

ΔY = grid spacing in y-dirction

$\Delta\tau$ = time increment

∇^2 = Laplacian operator $= \dfrac{\partial^2}{\partial X^2} + \dfrac{\partial^2}{\partial Y^2}$

ζ = dimensionless vorticity

γ = kinematic viscocity

μ = viscocity

τ = dimensionless time

ψ = streamfunction

β = volume expansion coefficient

ρ = density

θ_0 = initial temperature

θ_h = temperature along the hot wall

θ_c = temperature along the cold wall

Subscripts

i, j = space subscripts of grid points in X and Y directions

Superscripts

m = iteration number

n = time step

REFERENCES

[1] Alcharr S., Vasseur P., and Bilgen E., Natural Convection Heat Transfer in a Rectangular Enclosure with a Transverse Magnetic Field, *Transactions of ASME. J. Heat Transfer*, **117**, (1995), 668-673.

[2] Crammer K. R., and Pai S. I., *Magnetofluid Dynamics for Engineers and Applied Physicists*, Scripta Publishing Company, Washington, D.C., (1973),

[3] DeVahl Davis G., Laminar Natural Convection in an Enclosed Rectangular Cavity, *Int. J. Heat mass Transfer*, **11**, (1968), 1675-1693.

[4] Davis G., Natural Convection of Air in a Square Cavity: A Bench Mark Numerical Solution, *Int. J. Numer. Methods Fluids*, **3**, (1983), 249-264.

[5] Deng Q., Tang G., and Li Y., A Combined Temperature Scale for Analyzing Natural Convection in Rectangular Enclosures with Discrete Wall Heat Sources, *Int. J. Heat Mass Transfer*, **45**, (2002), 3437-3446.

[6] Frederick R. L., and Quiroz F., On Transition from Conduction to Convection in a Cubical Enclosure with a Partially Heated Walls, *Int. J. Heat and Mass Transfer*, **44**, (2001), 1699-1709.

[7] Nithyadevi N., Kandaswamy P., and Lee J., Natural Convection in a Rectangular Cavity with Partially Active Side Walls, *Int. J. Heat Mass Transfer*, **50**, (2007), 942-948.

[8] Kandaswamy P., Malliga Sundari S., and Nithyadevi N., Magneto Convection in an Enclosure with Partially Active Vertical Walls, **51**, (2008), 1946-1954.

[9] Mazumdar H. P., Ganguly U. N., and Venkataraman S. K., Some Effects of a Magnetic Field on the Flow of a Newtonian Fluid Through a Circular Tube, *Indian J. Pure and Applied Math.*, **27**(5), (1996), 519-524.

[10] Moreau R., *Magneto Hydrodynamics*, Kluwer Academic Publishers, The Netherlands, (1990).

[11] Ozoe H., and Maruo E., Magnetic and Natural Convection of Melted Silicon – Two Dimensional Numerical Computations for the Rate of Heat Transfer, *JSME*, **30**, (1987), 774-784.

[12] Ozoe H., and Okada K., The Effect of Direction of External Magnetic Field on the Three Dimensional Natural Convection in a Cubical Enclosure, *Int. J. Heat Mass Transfer*, **32**, (1989), 1939 -1954.

[13] Poots G., Heat Transfer by Laminar Free Convection in Enclosed Gas Layers, *Quart. J. Mech. Appl. Math.*, **11**, (1958), 257-273.

[14] Rudraiah N., Venkatachallappa M., and Subbaraya C. K., Combined Surface Tension and Buoyancy-Driven Convection in a Rectangular Open Cavity in the Presence of a Magnetic Field, *Int. Jour. Non-Linear Mechanics*, **35**, (1995b), 1-11.

[15] Sathiyamoorthy M., Tanmay Basak, Roy S., and Pop I., Steady Natural Convection Flows in a Square Cavity with Linearly Heated Side Walls, *Int. J. Heat and Mass Transfer*, **50**, (2007), 766-775.

[16] Vasseur P., Hasnaoui M., and Bilgen E., Natural Convection in an Inclined Fluid Layer with a Transverse Magnetic Field: Analogy with a Porous Medium, *Trans. ASME. J. Heat Transfer*, **117**, (1995), 121-129.

[17] Venkatachallappa M., and Subbaraya C. K., Natural Convection in a Rectangular Enclosure in the Presence of a Magnetic Field with Uniform Heat Flux from the Side Walls, *Acta Mechanica*, **96**, (1993), 13-26.

[18] Wilkes J. O., and Churchill S. W., The Finite Difference Computation of Natural Convection in a Rectangular Enclosure, *A.I.Ch.E. Journal*, **12**(1), (1966), 161-166.

S. Gokila
Department of Mathematics,
Coimbatore Institute of Technology,
Coimbatore, Tamilnadu-641 014, India.

V. Selladurai
Department of Mechanical Engineering,
Coimbatore Institute of Technology,
Coimbatore, Tamilnadu-641 014, India.
E-mail: beegee72002@yahoo.co.in